NO-REFERENCE PERCEPTUAL BLUR MODEL BASED ON INHERENT SHARPNESS

*Seungchul Ryu and *Kwanghoon Sohn*

Digital Image Media Lab (DIML)
Department of Electrical and Electronic Engineering, Yonsei University, Seoul, Republic of Korea
E-mail: {ryus01, *khsohn}@yonsei.ac.kr

ABSTRACT

An objective blurriness model is useful in various image processing applications. Especially, a no-reference model is expected as a highly desirable approach due to its applicability to wide range of applications. Blurriness of an image is known as to be commonly induced by the attenuation of spatial high-frequency and thus most conventional researches focused on a model estimating the amount of spatial high-frequency. However, the human-perceived blurriness might be varied across image contents. Very few researches have been investigated the human visual system model for the blurriness perception. To address the lack of an efficient model, this paper presents the blurriness perception model designed as a spatially varying function based on the inherent sharpness. Pixel-wise perceptual blurriness is computed employing the blurriness perception model and then integrated into an overall blurriness index using saliency information. The experimental comparisons with state-of-the-arts blurriness models for extensive public databases show that the proposed model is well-correlated with the subjective scores across different content of images, and outperforms the compared models.

***Index Terms*—** inherent sharpness, perceptual blur model, no-reference, blurriness perception model

1. INTRODUCTION

The ability to quantify the perceived blurriness of an image is useful in various image processing applications, such as super-resolution, deblurring, and image fusion [1, 2, 3]. For example, an objective blurriness index can be used to adjust parameters or iterations in deblurring algorithms. Blurriness score is also availabe to ascertain the overall quality of an image possibly combined with other factors [4, 5].

A subjective human assessment is considered the most reliable method for evaluating the perceived blurriness of an image, since human beings are commonly end users in many applications. However, subjective methods are very time-consuming and expensive, and thus are impractical for real-time applications. Instead, an objective assessment has been expected to substitute for a subjective method due to its low-complexity and consistency. Based on the amount of reference information needed, objective image quality assessments are classified into three categories: full-reference, reduced-reference, and no-reference methods [6]. The no-reference method, among them, is the most desirable approach since in many applications the reference image is unavailable.

It is well known that the attenuation of high-frequency elements causes an image to appear blurred, i.e., the degree of a perceived blurriness is inversely proportional to the amount of spatial high-frequency. However, the human visual system (HVS) differently perceives the blurriness of images containing the same amount of spatial high-frequency across image contents. Given the phenomenon, the perceptual blurriness, B, can be modeled as $B = \Psi\left(|e_h|_a\right)$ where e_h is spatial high-frequency elements, $|\cdot|_a$ means the amount of e_h, and Ψ is the HVS model for blurriness perception.

In recent decades, a lot of no-reference blurriness models have been proposed. Majority of the models were only focused on estimating $|e_h|_a$ and did not consider the HVS, i.e., the function Ψ is assumed as a trivial linear function. To estimate $|e_h|_a$, derivative information was used in the electron microscopy field [7], and also employed in more recent literature [8, 9]. Edge information, especially the width of an edge, is also employed as a key factor to estimate the amount of high-frequency $|e_h|_a$ [5, 10, 11]. $|e_h|_a$ can be estimated in a transform domain, for example, the method presented in [12] is based on the summation of frequency component magnitudes above a threshold. In [13], $|e_h|_a$ is measured using discrete cosine transform (DCT) coefficient that are close to zero. In [14, 15], a kurtosis in the frequency domain, which is a statistical measure of the peakedness of a distribution, is employed as an index for estimating $|e_h|_a$.

These approaches can estimate blurriness well within a single image content, but cannot be applicable for image-across blurriness estimation because HVS-perceived blurriness is varied according to the content of an image. To address this problem, a few number of studies explored the HVS model Ψ for the blurriness perception. Ferzli and Karam [16] proposed a probability summation model based on the concept of just noticeable blur (JNB) as Ψ. The perceived sharpness[1] is estimated by integrating local blurriness scores with the JNB model. Several extensions of this method [17, 18] have been studied in order to settle its defects. In [17], the authors proposed an iterative edge refinement algorithm to solve the inaccuracy problem for over-blurred images. In [18], Narvekar *et al.* utilized a probabilistic model to estimate the probability of detecting blur at each edges in an image. Then, a blur index was computed by pooling the probabilities at each edges via the cumulative probability of blur detection (CPBD) method.

Even though edge information is a good index for measuring blurriness, the use of these algorithms is limited since edges are remarkably different from image to image. Especially, their performance drastically decreases for edgeless images. In our previous work [19], a sharpness index was proposed based on the image content adaptive Ψ model. However, in [19], local characteristics of an image were not considered; instead, only global features were used to estimate the perceived image sharpness. Similar to [19], most

(*): corresponding author

[1] Sharpness is the antonym of blurriness and in common inversely proportional to blurriness.

blurriness models are suitable for quantifying the overall blurriness of an image, not for providing local blurriness map[2], which is useful in certain applications [20].

Based on the concept of inherent sharpness presented in [19], we model Ψ as a spatially varying function which depends on image contents, named as inherent sharpness model (ISM). Perceptual pixel-wise blurriness is computed using ISM and $|e_h|_a$ estimated in wavelet domain. The pixel-wise blurriness are integrated into an overall image blurriness index with visual saliency information. Also, this pixel-wise blurriness map has potential to be used in space-variant image processing. The remainder of this paper is organized as follows. Section 2 describes the proposed model in detail. Section 3 presents experimental evaluations of the proposed method with comparisons to state-of-the-art methods, and discusses about possible applications. Lastly, Section 4 concludes this paper with future works.

2. NO-REFERENCE PERCEPTUAL BLUR MODEL BASED ON INHERENT SHARPNESS

As described in the previous section, the perceptual blurriness, B, can be modeled as $B = \Psi\left(|e_h|_a\right)$ where e_h is spatial high-frequency elements, $|\cdot|_a$ means the amount of e_h, and Ψ is the HVS model for the blurriness perception. This section describes how the proposed no-reference blur model estimates B in detail. In the method, $|e_h|_a$ is estimated using diagonal-detailed sub-signal in wavelet domain and Ψ is modeled using the concept of inherent sharpness and visual saliency information. First, pixel-wise spatial high-frequency elements $|e_h(\mathbf{p})|_a$ for each pixel position $\mathbf{p}$ is computed in wavelet domain. Second, pixel-wise perceptual blurriness $b(\mathbf{p})$ are computed with ISM. Lastly, $b(\mathbf{p})$ are integrated into an image blur index using visual saliency $\mathbf{s}$. Detailed descriptions for each steps are given in the followings.

To study how the HVS perceives blurriness (or sharpness) across image contents, in our previous work [19], subjective experiments were conducted with various spatial complexity of images. In the experiment, six images selected from LIVE image database [21] were cropped into smaller ones (255 by 175) to obtain test images containing different complexity: three of test images have low spatial complexity while the other three have high spatial complexity. The undistorted images were blurred by a 7×7 Gaussian kernel with standard deviations of 0.5, 1.0, 1.5, 2.0 and 2.5. 36 test images were used overall for the experiment. 15 subjects evaluated test images in terms of sharpness using the absolute category rating (ACR) with five grades: very blurred, blurred, non-blurred, sharp, and very sharp. Then 15 scores for each image were averaged to obtain mean opinion scores (MOS).

The results of the experiment are shown in Fig. 1, which describes a relationship between $|e_h|_a$ and the perceived sharpness (MOS) for different complexity of images. Here, $|e_h|_a$ was computed by the L_2 norm of high-frequency above the cutoff frequency of $\pi/8$ in Fourier domain. As shown in Fig. 1, the perceived sharpness increased, as $|e_h|_a$ incremented, within an image group for both low complexity images and high complexity images. However, across image complexity, the perceived sharpness discrepancy is induced by the fact that an image complexity itself influences on the perceived sharpness. We define the factor causing the perceived sharpness discrepancy as *inherent sharpness*. If inherent sharpness

[2]Although it is possible to modify existing blurriness models to generate a blurriness map in a block-based method, the accuracy and reliability are very limited [20].

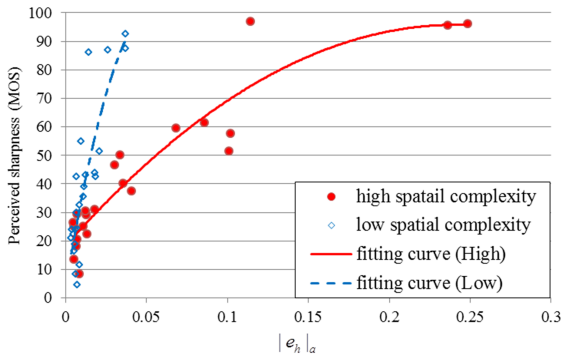

Fig. 1. Relationship between $|e_h|_a$ and the perceived sharpness (MOS) for different image groups of low and high spatial complexity

term, which is content dependent, is eliminated, only a content independent factor is remained. The content independent factor is named as perceptual blurriness b and computed by ISM as follows:

$$b(\mathbf{p}) = \frac{\chi(\mathbf{p})}{|e_h(\mathbf{p})|_a + c}, \tag{1}$$

where $c = 0.01$ is a constant for stability and $\chi(\mathbf{p})$ is the function for measuring a spatial complexity of an image. Gaussian weighted morphological gradients is used as $\chi(\mathbf{p})$ in this paper, but any proper function can be used. $\chi(\mathbf{p})$ is defined as follows:

$$\chi(\mathbf{p}) = \sum_{\mathbf{p}\in W_\chi} g(\mathbf{p}) \cdot m(\mathbf{p}), \tag{2}$$

$$m(\mathbf{p}) = \max\Omega(\mathbf{p}) - \min\Omega(\mathbf{p}), \tag{3}$$

$$\Omega(\mathbf{p}) = \left\{X(\mathbf{p}+\Delta)|\Delta \in N^2, |\Delta| \le 1\right\}, \tag{4}$$

where $g(\mathbf{p})$ is Gaussian weight, m($\mathbf{p}$) is a morphological gradient, W_χ is a 64×64 window, and X is an input image.

In the proposed method, pixel-wise spatial high-frequency $|e_h(\mathbf{p})|_a$ is computed in wavelet domain. The wavelet transform is an effective way to determine both spatial and frequency properties and thus is suitable for estimating pixel-wise high-frequency information. $|e_h(\mathbf{p})|_a$ is defined as follows:

$$|e_h(\mathbf{p})|_a = \sum_{\mathbf{p}\in W_\omega} g(\mathbf{p}) \cdot \omega_D(\mathbf{p}), \tag{5}$$

where $g(\mathbf{p})$ and W_ω are Gaussian weight and a 64×64 window, respectively. ω_D is a diagonal detailed wavelet sub-signal defined as follows:

$$\omega_D(\mathbf{p}) = \sum_{\mathbf{n}} \varphi_D(\mathbf{p}) \cdot X(\mathbf{n}), \tag{6}$$

where φ_D is a diagonal wavelet function composed of two impulse responses of horizontal and vertical high-pass filters. Note that the Haar wavelet is used in this paper due to its simplicity, but any alternative wavelet can be used if it can provide diagonal elements.

The HVS generally lends more attention to salient regions, such as an edge, a local contrast, and an object [22]. Thus, distortions presented in attended regions are more frequently perceived by the HVS. We used such saliency information to derive an overall blurriness index of an image from the local blurriness scores. In this paper, graph-based visual saliency (GBVS) [23] is employed. A bottom-up visual saliency model, GBVS, is based on random walks on the graphs constructed using the edge strengths between two

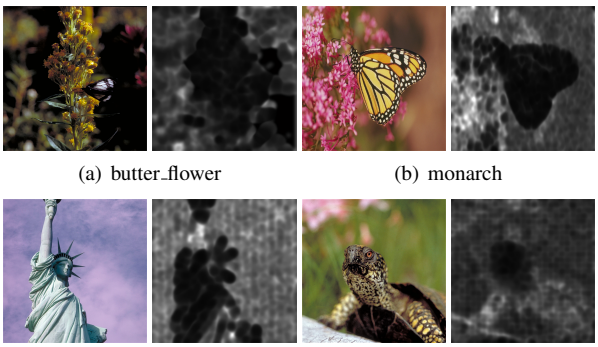

(a) butter_flower (b) monarch

(c) lady_liberty (d) turtle

Fig. 2. Local perceptual blurriness maps for images containing spatially varied blurriness: (a) butter_flower, (b) monarch, (c) lady_liberty, and (d) turtle.

nodes. Note that any other visual saliency model (e.g. [24, 25]) can replace the GBVS in the proposed model if it can provide a pixel-wise saliency map.

The perceptual blurriness index B of an image is computed using pixel-wise perceptual blurriness b($\mathbf{p}$) and pixel-wise saliency information s($\mathbf{p}$) as follows:

$$B = \log_{10}\left(K \cdot \sum_{\mathbf{p}} b(\mathbf{p}) \cdot s(\mathbf{p})\right), \tag{7}$$

where $K = \sum_{\mathbf{p}} s(\mathbf{p})$ is a normalization factor. Logarithmic mapping is employed in (7) in order to account for the nonlinear perception in HVS. Substituting for $b(\mathbf{p})$ in (7) from (1) one obtains

$$\begin{aligned} B &= \Psi(|e_h|_a) \\ &= \log_{10}\left(K \cdot \sum_{\mathbf{p}} \frac{\chi(\mathbf{p})}{|e_h(\mathbf{p})|_a + c} \cdot s(\mathbf{p})\right). \end{aligned} \tag{8}$$

where $\chi(\mathbf{p})$ and $|e_h(\mathbf{p})|_a$ are computed by (2) and (5), respectively. B increases as blurriness of an image rises and is always nonnegative, i.e., a value of that is closer to zero indicates a sharper image. The MATLAB implementation of the proposed model is available in [26].

3. PERFORMANCE EVALUATIONS AND APPLICATIONS

This section presents the experimental results for the proposed perceptual blur model and discusses about other applications. The performance evaluation in assessing blurred image quality using six publicly available image databases is given in Section 3.1, and possible applications of the proposed blur model are discussed in Section 3.2.

3.1. Quality assessment of blurred images

To evaluate the performance of the proposed model in assessing the quality of blurred images, six public image databases, DIML [19], LIVE [21], TID2008 [27], IVC [28], CSIQ [29], and A57 [30] databases were used. The DIML database [19] consists of ten original images and 150 distorted images by JPEG-2000, Gaussian blur, and motion blur at five distortion levels. The subjective experiments were conducted according to ITU-R BT.500 recommendations [31]. In the experiments, ten subjects graded each image in terms of the perceived sharpness using continuous scale. Test images were randomly displayed on a LG FLATRON E2350 high-resolution LCD monitor, and the final MOS for each image was computed by averaging the grades given by ten subjects. All the images, including the Gaussian blurred, motion blurred, and JPEG-2000 compressed images, were used in our experiments.

The LIVE [21] database consists of 29 original color images and 982 distorted images. The distortion types are JPEG-2000, JPEG, Gaussian blur, white noise, and transmission error. The subjective experiments were conducted using a continuous linear scale with 20-29 subjects. The difference mean opinion score (DMOS) for each image was then calculated from the raw scores. All of the Gaussian-blurred images (174 images) and all of the JPEG-2000 compressed images (227 images) from the LIVE database were used in our experiments.

The TID2008 database [27] consists of 25 original images and 1700 distorted images. The distortion types comprise 17 different distortions at four distortion levels, including JPEG-2000, Gaussian blur, denoising, JPEG, impulse noise, and mean shift. In our experiments, all of the Gaussian blurred natural images (96 images), all of the JPEG-2000 compressed natural images (96 images), and all of the denoising natural images (96 images) from the TID2008 database were used.

The IVC database [28] consists of 10 original images and 235 distorted images. The distortion types are JPEG, JPEG2000, Locally Adaptive Resolution (LAR) coding, and Gaussian blurring. The subjective experiments were conducted using a double stimulus impairment scale method (DSIS) with fifteen subjects. In our experiments, all of the Gaussian-blurred images (24 images) and all of the JPEG2000 compressed images (60 images) were used.

The CSIQ database [29] consists of 30 original images and 866 distorted images. The distorted images comprise six different types of distortions at four to five distortion levels, including JPEG, JPEG2000, global contrast decrements, additive white Gaussian noise, additive pink Gaussian noise, and Gaussian blurring. Twenty-five subjects participated in the subjective experiments. All of the Gaussian blurred images (180 images) and JPEG-2000 compressed images (180 images) were used in our experiments.

The A57 database [30] consists of 3 original images and 54 distorted images. The distortion types are JPEG, JPEG-2000, additive white Gaussian noise, Gaussian blur, Dynamic Contrast-based Quantization (DCQ), and LH sub-bands quantization. The subjective experiments were conducted using a continuous scale in which each distorted image was rated against the original image. In our experiments, all of the Gaussian blurred images (ten images), all of the JPEG-2000 compressed images (ten images) and all of the DCQ compressed images (ten images) were used.

The distortion types of the blurred test images are Gaussian blur (534 images), JPEG-2000 compression (623 images), motion blur (50 images), DCQ compression (10 images), and denoising (96 images). In all, 1313 images are employed in our evaluation. For the evaluation, we follow the suggestions of the VQEG report [32]. A four parameter logistic function, as recommended in [32], is used for non-linear regression before calculating the performance measures. The logistic function used is as follows:

$$MOS_{pi} = \frac{\beta_1 - \beta_2}{e^{(S_i - \beta_3)/|\beta_4|} + 1} + \beta_2, \tag{9}$$

where β_1, β_2, β_3, and β_4 are model parameters, MOS_{pi} is the predicted MOS, and S_i is the score of the model. The values of β_1, β_2, β_3, and β_4 are first obtained by fitting to the corresponding sub-

Table 1. PCC comparisons for each database. The bold numbers indicate the top and the second highest PCCs for each database.

Database	Proposed	GISM [19]	JNBM [16]	EWM [5]	CPBD [18]	DCT [13]	Kurtosis [14]	EPM [15]
DIML	**0.918**	**0.892**	0.742	0.751	0.886	0.721	0.868	0.720
LIVE	**0.893**	0.810	0.785	0.814	**0.905**	0.824	0.818	0.834
TID2008	**0.894**	**0.886**	0.848	0.846	0.885	0.839	0.856	0.763
IVC	**0.879**	0.782	0.606	0.586	0.755	0.724	0.691	**0.823**
CSIQ	**0.871**	0.776	0.825	0.841	**0.859**	0.834	0.813	0.810
A57	**0.835**	0.784	**0.834**	0.792	0.734	0.722	0.813	0.675
Average	**0.738**	0.641	0.674	0.677	0.646	0.664	**0.704**	0.621

jective MOS scores, and then MOS_{pi} is calculated. The MOS_{pi} are used in calculating the performance measures, including Pearsons correlation coefficient (PCC, which indicates the prediction accuracy), the Spearman rank-order correlation coefficient (SROCC, which indicates the prediction monotonicity), the root mean squared error (RMSE, which indicates the prediction consistency), and the mean absolute error (MAE, which indicates the prediction consistency). Note that for a well-designed model, the values of PCC and SROCC should be high, and the values of RMSE and MAE should be low.

The proposed model is evaluated by comparisons with several no-reference blurriness/sharpness measuring models: the global inherent sharpness based model (GISM) [19], just noticeable blur based model (JNBM) [16], edge width based model (EWM) [5], cumulative probability of blur detection based model (CPBD) [18], DCT based model (DCT) [13], kurtosis based model (Kurtosis) [14], and edge profile based model (EPM) [15].

Tables 1 summarizes PCC comparisons of the models for each database. As seen in Table 1, the proposed model shows good performance for all the databases, and outperforms the other models for most cases. Actually, the proposed model provides the highest correlations for all databases except for LIVE database (the second-top performance for LIVE database). The objective performance measures (PCC, SROCC, RMSE, and MAE) for all the images from six databases are presented in Table 2. PCC, SROCC, RMSE, and MAE in Table 2 are average of values for each database. The proposed model shows the highest PCC and SROCC, which indicate the prediction accuracy and monotonicity. Although RMSE and MAE of the proposed model are not the lowest, the performance is still competitive. More comparisons analyzing the performance for each distortion type were provided in supplementary document at [26]. The experimental analysis shows that the proposed model is reliable and consistent with correlating well to subjective scores, thus can be considered as an effective perceptual blurriness index in no-reference applications.

3.2. Other applications

Besides application to the quality assessment of blurred images, the proposed model is useful for other tasks: general image quality assessment with other distortions, local blurriness prediction, and spatial variant image processing. Blurriness is the most common distortion in typical image processes, such as acquisition, compression, denoising, up-sampling, and so on. Nevertheless, other distortions can occur in several applications. For example, the blocking artifact is one of the dominant distortions in JPEG compressed images [33], while the ringing artifact is one of the dominant distortions in JPEG-2000 compressed images [34]. Gaussian noise and pack-loss are also typical distortions that generally occur in image transmission [35]. Accordingly, the perceptual blurriness measured using the proposed model can be used to predict the perceptual quality of images with combined to other distortions.

Furthermore, the proposed model can provide a local blurriness map which is useful for a variety of applications, e.g., locally adaptive deblurring [36], multi-focus image fusion [37], and the classification of blurry or non-blurry regions [38, 39]. In Fig. 2, local perceptual blurriness maps for images containing spatially variant blurriness are presented in which brighter pixels represent more blurred regions. In the figures, sharp foreground objects are clearly distinguished from the blurry background scenes. The results imply that blurriness maps can be used to classify an image into blurry or non-blurry regions. The local blurriness can also be used as one of the features in an image segmentation algorithm. Also, locally adaptive image processing such as deblurring and enhancement can be conducted with the local blurriness map.

4. CONCLUSION

This paper proposes an objective no-reference perceptual blur model employing HVS perception model designed using ISM and visual saliency. Pixel-wise perceptual blurriness is computed by ISM and diagonal wavelet sub-signal, then integrated into overall blurriness index with visual saliency. An experimental analysis of the proposed method for extensive public databases shows that the proposed model performs well in assessing the quality of blurred images and outperforms the compared state-of-the-art models. Furthermore, the proposed method provides a local blurriness map which is useful for many applications, such as locally adaptive image processing, blurry region detection, and multi-focus image fusion. Future works include extending the proposed model to stereo images considering a binocular perception of blurriness. Other directions for future works include the development of spatially adaptive deblurring and blurry region-based image segmentation.

Table 2. PCC, SROCC, RMSE, MAE comparisons for all images from six databases. The bold numbers indicate the top performance.

	PCC	SROCC	RMSE	MAE
Proposed	**0.851**	**0.839**	6.99	5.73
GISM [19]	0.805	0.792	6.99	5.51
JNBM [16]	0.748	0.715	6.73	4.46
EWM [5]	0.754	0.743	5.76	4.24
CPBD [18]	0.820	0.801	5.50	5.04
DCT [13]	0.762	0.744	6.11	6.08
Kurtosis [14]	0.795	0.735	**4.72**	**3.72**
EPM [15]	0.750	0.721	5.49	4.34

5. REFERENCES

[1] D. Rajan and S. Chaudhuri, "Simultaneous estimation of super-resolved scene and depth map from low resolution defocused observations," *IEEE Transactions on Pattern Analysis and Machine Intelligence*, vol. 25, no. 9, pp. 1102-1117, Sep. 2003.

[2] X. Zhu and P. Milanfar, "Automatic parameter selection for denoising algorithms using a no-reference measure of image content," *IEEE Transactions on Image Processing*, vol. 19, no. 12, pp. 3116-3132, Dec. 2010.

[3] S. Soleimani, F. Rooms, W. Philips, and L. Tessens, "Image fusion using blur estimation," *in Proc. IEEE International Conference on Image Processing (ICIP)*, Hong Kong, Hong Kong, Sep. 2010.

[4] Z. Wang, H. R. Sheikh, and A. C. Bovik, "No-reference perceptual quality assessment of JPEG compressed images," *in Proc. IEEE International Conference on Image Processing (ICIP)*, Rochester, NY, USA, Sep. 2002.

[5] P. Marziliano, F. Dufaux, S. Winkler, and T. Ebrahimi, "Perceptual blur and ringing metrics: application to JPEG2000," *Signal Processing: Image Communication*, vol. 19, no. 2, pp. 163-172, Feb. 2004.

[6] Z. Wang and A. C. Bovik, Modern Image Quality Assessment, *Morgan & Claypool*, USA, 2006.

[7] L. Firestone, K. Cook, K. Culp, N. Talsania, and J. Preston, "Comparison of autofocus methods for automated microscopy," *Cytometry*, vol. 12, no. 3, pp. 195-206, 1991.

[8] L. Liang, J. Chen, S. Ma, D. Zhao, and W. Gao, "A no-reference perceptual blur metric using histogram of gradient profile sharpness," *in Proc. IEEE International Conference on Image Processing (ICIP)*, Cairo, Egypt, Nov. 2009.

[9] M. J. Chen, A. C. Bovik, "No-reference image blur assessment using multiscale gradient," *EURASIP Journal on Image and Video Processing*, vol. 2011, no. 1, pp.1-11, Jul. 2011.

[10] P. Marziliano, F. Dufaux, S. Winkler, and T. Ebrahimi, "A no-reference perceptual blur metric," *in Proc. IEEE International Conference on Image Processing (ICIP)*, Rochester, NY, USA, Sep. 2002.

[11] E. Ong, W. Lin, Z. Lu, X. Yang, S. Yao, F. Pan, L. Jiang, and F. Moschetti, "A no-reference quality metric for measuring image blur," *in Proc. International Symposium on Signal Processing and Its Applications*, Paris, France, Jul. 2003.

[12] T. Cover and J. Thomas, Elements of information theory, *Wiley Series*, 1991.

[13] X. Marichal, W. Y. Ma, and H. J. Zhang, "Blur determination in the compressed domain using DCT information," *in Proc. IEEE International Conference on Image Processing (ICIP)*, Kobe, Japan, Oct. 1999.

[14] N. Zhang, A. Vladar, M. Postek and R. Larrabee, "Spectral density-based statistical measures for image sharpness," *Metrologia*, vol. 42, no. 5, pp. 351-359, Aug. 2005.

[15] J. Caviedes and F. Oberti, "A new sharpness metric based on local kurtosis, edge and energy information," *Signal Processing: Image Communication*, vol. 19, no. 2, pp. 147-161, Feb. 2004.

[16] R. Ferzli and L. J. Karam, "A no-reference objective image sharpness metric based on the notion of just noticeable blur (JNB)," *IEEE Transaction on Image Processing*, vol. 18, no. 4, pp. 717-728, Arp. 2009.

[17] S. Varadarajan and L. J. Karam, "An improved perception-based no-reference objective image sharpness metric using iterative edge refinement," *in Proc. IEEE International Conference on Image Processing (ICIP)*, San Diego, CA, USA, Oct. 2008.

[18] N. D. Narvekar and L. J. Karam, "A no-reference image blur metric based on the cumulative probability of blur detection (CPBD)," *IEEE Transactions on Image Processing*, vol. 20, no. 9, pp. 2678-2683, Sep. 2011.

[19] S. Ryu and K. Sohn, "No-reference sharpness metric based on inherent sharpness," *Electronics Letters*, vol. 47, no. 21, pp. 1178-1180, Oct. 2011.

[20] C. T. Vu, T. D. Phan, and D. M. Chandler, "S_3: A spectral and spatial measure of local perceived sharpness in natural images," *IEEE Transacions on Image Processing*, vol. 21, no. 3, pp. 934-945, Mar. 2012.

[21] H. R. Sheikh, LIVE Image Quality Assessment Database, Release 2, 2005. [Online]. Available: http://live.ece.utexas.edu/research/quality.

[22] N. Bruce and J. K. Tsotsos, "Saliency, attention, and visual search: An information theoretic approach," *Journal of Vision*, vol. 9, no. 3, pp. 1-24, Mar. 2009.

[23] J. Harel, C. Koch, and P. Perona, "Graph-based visual saliency," *Advances in Neural Information Processing Systems*, vol. 19, pp. 525-552, 2007.

[24] S. Ryu, B. Ham, and K. Sohn, "Contextual information based visual saliency model," in *Proc. IEEE International Conference on Image Processing (ICIP)*, Melbourne, Australia, Sep. 2013.

[25] J. Li, M. Levine, X. An, X. Xu, and H. He, "Visual saliency based on scale-space analysis in the frequency domain," *IEEE Transactions on Pattern Analysis and Machine Intelligence*, vol. 35, no. 4, pp. 996-1010, Apr. 2013.

[26] http://diml.yonsei.ac.kr/∼sryu/lism/.

[27] N. Ponomarenko, Tampere Image Database 2008 version 1.0, 2008. [Online]. Available: http://www.ponomarenko.info/tid2008.htm.

[28] P. Le Callet, Subjective Quality Assessment IRCCyN/IVC Database, 2005. [Online]. Available: http://www.irccyn.ec-nantes.fr/ivcdb/.

[29] D. M. Chandler, CSIQ Image Database, 2010. [Online]. Available: http://vision.okstate.edu/index.php?loc=csiq.

[30] D. M. Chandler and S. S. Hemami, A57 Database, 2007. [Online]. Available: http://foulard.ece.cornell.edu/dmc27/vsnr/vsnr.html.

[31] ITU-R Recommendation BT.500-11, "Methodology for the subjective assessment of the quality of television pictures," ITU-R, Geneva, Switzerland, 2000.

[32] VQEG, "Final report from the Video Quality Experts Group on the validation of objective models of video quality assessment Phase II," Aug. 2003.

[33] S. Ryu and K. Sohn, "Blind blockiness measure based on marginal distribution of wavelet coefficient and saliency," *in Proc. IEEE International Conference on Acoustics, Speech, and Signal Processing (ICASSP)*, Vancouver, Canada, May 2013.

[34] H. Liu, N. Klomp, and I. Heynderickx, "A no-reference metric for perceived ringing artifacts in images," *IEEE Transactions on Circuits and Systems for Video Technology*, vol. 20, no. 4, pp. 529-539, Apr. 2010.

[35] A. Khan, L. Sun, and E. Ifeachor, "QoE prediction model and its applications in video quality adaptation over UMTS networks," *IEEE Transactions on Multimedia*, vol. 14, no. 2, pp. 431-442, Apr. 2012.

[36] H. Takeda, S. Farsiu, and P. Milanfar, "Deblurring using regularized locally adaptive kernel regression," *IEEE Transactions on Image Processing*, vol. 17, no. 4, pp. 550-563, Apr. 2008.

[37] J. Tian, L. Chen, L. Ma, and W. Yu, "Multi-focus image fusion using a bilateral gradient-based sharpness criterion," *Optics Communications*, vol. 284, no. 1, pp. 80-87, Jan. 2011.

[38] B. Su, S. Lu, and C. L. Tan, "Blurred image region detection and classification," *in Proc. ACM International Conference on Multimedia (MM)*, Sottsdale, AZ, USA, Nov. 2011.

[39] R. Liu, Z. Li, and J. Jia, "Image partial blur detection and classification," *in Proc. IEEE Conference on Computer Vision and Pattern Recognition(CVPR)*, Anchorage, AK, USA, Jun. 2008.